

# A unique gravitational wave signal from phase transition during inflation

Haipeng An,<sup>1,2</sup> Kun-Feng Lyu,<sup>3,4</sup> Lian-Tao Wang,<sup>5,6</sup> and Siyi Zhou<sup>7</sup>

<sup>1</sup>*Department of Physics, Tsinghua University, Beijing 100084, China*

<sup>2</sup>*Center for High Energy Physics, Tsinghua University, Beijing 100084, China*

<sup>3</sup>*Department of Physics, the Hong Kong University of Science and Technology, Clear Water Bay, Kowloon, Hong Kong S.A.R., P.R.C.*

<sup>4</sup>*Kavli Institute for Theoretical Physics, University of California, Santa Barbara, CA 93106, USA*

<sup>5</sup>*Department of Physics and Enrico Fermi Institute, University of Chicago, Chicago, IL 60637, USA*

<sup>6</sup>*Kavli Institute for Cosmological Physics, University of Chicago, Chicago, IL 60637, USA*

<sup>7</sup>*The Oskar Klein Centre for Cosmoparticle Physics & Department of Physics, Stockholm University, AlbaNova, 106 91 Stockholm, Sweden*

We study the properties of the gravitational wave (GW) signals produced by first order phase transitions during the inflation era. We show that the power spectrum of the GW oscillates with its wave number. This signal can be observed directly by future terrestrial and spatial gravitational wave detectors and through the B-mode spectrum in CMB. This oscillatory feature of GW is generic for any approximately instantaneous sources occurring during inflation, and is distinct from the GW from phase transitions after the inflation. The details of the GW spectrum contain information about the scale of the phase transition and the later evolution of the universe.

**Introduction** Gravitational waves (GWs), once produced, propagate freely through the universe and can bring us the information of their origin and the history of the universe. They can be detected in many proposed, either terrestrial or space based, detectors [1–16]. Primordial GWs can also leave hints on the cosmological microwave background (CMB) and can be detected in the B-mode power spectrum [17–19]. Possible sources of the primordial GWs are inflation [20–24], first order phase transitions [25, 26], and cosmic strings [27–32].

It is highly plausible that there was an inflationary era in early universe [33–35] (See Ref. [36]). The simplest inflation model is driven by a slow rolling inflaton. To produce enough inflation, the typical excursion of the inflaton field must be large. As such, it may induce significant changes in the dynamics of the spectator fields. This may happen through a direct coupling between the inflaton field to other spectator fields (see, e.g., Ref. [37]). The change in temperature during inflation is another possibility (see Refs. [38, 39] as examples). Such changes can trigger dramatic events during inflation, such as a first order phase transition [40, 41].

In this letter, we show that the GWs produced by bubble collisions in first order phase transition during inflation can provide a unique *oscillatory* signal in its power spectrum, which contains information of both inflation and the phase transition. It should be clear from the discussion below that the signal is generic for approximately instantaneous GW sources.

**GWs from local and instantaneous sources.** The equation of motion for the transverse and traceless GW perturbation  $h_{ij}$  is

$$h''_{ij} + \frac{2a'}{a} h'_{ij} - \nabla^2 h_{ij} = 16\pi G_N a^2 \sigma_{ij}, \quad (1)$$

where ' indicates derivatives with respect to the conformal time  $\tau$ ,  $G_N$  is the Newton's gravity constant, and  $\sigma_{ij}$  is the transverse, traceless part of the energy momentum tensor. There are several important time scales in the problem:  $\tau_*$  is the time of bubble collision and generation of the GW. The inflation ends at  $\tau_{\text{end}}$ . We denote the conformal time duration and the co-moving spatial spread of the bubble collision event to be  $\Delta_{\tau,x}$ .  $\Delta_{\tau,x} \ll |\tau_*|$  by assumption for instantaneous and local sources that happened during inflation. The modes of interest to us are all outside the horizon at the time when inflation ends,  $k|\tau_{\text{end}}| \ll 1$ , where  $k$  is the co-moving momentum.

**Spectral shape of the GW signal.** We focus on three regimes with qualitatively different features.

- $|\tau_*|^{-1} < k < \Delta_{\tau,x}^{-1}$ . In this regime, we can ignore the spatial inhomogeneity caused by the bubbles and treat the bubble collisions as instantaneous sources. Therefore the bubble collisions can be approximated as delta function sources,

$$\tilde{\sigma}_{ij} \approx \tilde{T}_{ij}^{(0)} a^{-3}(\tau_*) \delta(\tau - \tau_*), \quad (2)$$

where  $\tilde{T}_{ij}^{(0)}$  is a constant depending on the strength of the source.

During inflation and after the bubble collision,  $|\tau_*| \gg |\tau| > |\tau_{\text{end}}|$ , we have (after Fourier transformation, and suppressed  $i, j$  indices)

$$\begin{aligned} \tilde{h}_k(\tau) \approx & -\frac{16\pi G_N H_{\text{inf}} \tilde{T}^{(0)} \tau}{k} \left[ \left( \frac{1}{k\tau} - \frac{1}{k\tau_*} \right) \cos k(\tau - \tau_*) \right. \\ & \left. + \left( 1 + \frac{1}{k^2(\tau\tau_*)} \right) \sin k(\tau - \tau_*) \right], \quad (3) \end{aligned}$$

where  $H_{\text{inf}}$  is the Hubble expansion rate. In position space, when  $k^2\tau\tau_* \ll 1$ ,  $h(\tau, \mathbf{x})$  is approximately

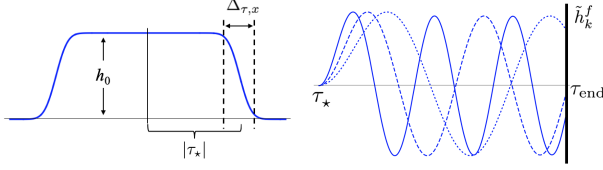


FIG. 1: Left: configuration of bound state of GW in the inflation era. Right: Fourier modes of GW during inflation from  $\tau_*$  to  $\tau_{\text{end}}$ .

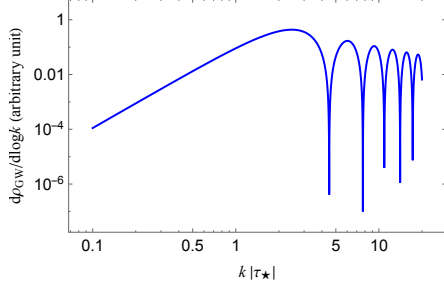


FIG. 2: Illustration of the shape of the GW spectrum produced by instantaneous source during inflation.

$4G_N H_{\text{inf}} \tilde{T}^{(0)} |\tau_*|^{-1} \Theta(\tau - \tau_* - |\mathbf{x} - \mathbf{x}_*|)$ , which is a uniform over density ball with radius  $|\tau_*|$ , as shown in the left panel of Fig. 1. At the end of inflation, the universe is filled with such GW balls. In this regime, we can ignore the terms suppressed by  $(k\tau_*)^{-1}$  in Eq. (3). After the production of the GW at  $\tau \approx \tau_*$ , it will continue to oscillate until it exits the horizon at  $k|\tau| \approx 1$  when its phase starts to freeze. The GW then evolves to the end of the inflation, and with  $k\tau_{\text{end}} \rightarrow 0$ , its value is frozen to

$$\tilde{h}_k^f = -\frac{16\pi G_N H_{\text{inf}} \tilde{T}^{(0)}}{k^2} \left( \cos k\tau_* - \frac{\sin k\tau_*}{k\tau_*} \right). \quad (4)$$

Since  $k|\tau_*| > 1$ , we can neglect the term proportional to  $\sin k\tau_*/k\tau_*$ . Hence,  $\tilde{h}_k^f \sim \cos k\tau_*$ , as shown in the right panel of Fig. 1.

The GW starts to oscillate again after re-entering the horizon, with  $\tilde{h}_k^f$  as the initial condition. For example, if we assume the universe evolves into the radiation domination (RD) immediately after inflation,

$$\tilde{h}_k(\tau) = \tilde{h}_k^f \times \frac{\sin k\tau}{k\tau}. \quad (5)$$

Hence,  $\tilde{h}_k(\tau) \propto \cos(k\tau_*)$ . The energy density of the GW has the form

$$\rho_{\text{GW}} \sim \frac{1}{a^2(\tau)} \int \frac{d^3k}{(2\pi)^3} |\tilde{h}_k'(\tau)|^2. \quad (6)$$

As a result, deeply inside the horizon ( $k\tau \gg 1$ ), we have

$$\frac{d\rho_{\text{GW}}}{d\log k} \sim \frac{1}{k} \left( \cos k\tau_* - \frac{\sin k\tau_*}{k\tau_*} \right)^2 \approx \frac{1}{k} \cos^2 k\tau_*. \quad (7)$$

We see that the GW has a distinct *oscillatory* feature in the frequency space, with a period of  $\pi/\tau_*$ . This feature stems from the instantaneous nature of the GW production, which sets up a GW spectrum proportional to  $\cos k|\tau_*|$  at the end of the inflation. The GW energy density also has an overall factor of  $k^{-1}$  [41], since the modes with longer wavelength redshift less before exiting the horizon. An illustration of the GW spectrum is shown in Fig. 2.

- $k < \tau_*^{-1}$ . In this regime, we can ignore the details of the GW source, and treat it as a delta function in space-time. Hence, Eq. (3) still applies. In the limit  $k|\tau_{\text{end}}| \ll k|\tau_*| \ll 1$ , from Eq. (4),  $\tilde{h}_k^f$  is independent of  $k$  at leading order. From Eq. (7) we have  $d\rho_{\text{GW}}/d\log k \propto k^3$ , also shown in Fig. 2, which is similar to the case of a point-like source in Minkowski space.

- $k \gtrsim \Delta_{\tau,x}^{-1}$ . In this regime, we have  $k|\tau_*| \gg 1$ . The details of the bubble collision become essential, and we will need numerical simulations to obtain the shape of the signal. At such small scales, the curvature of the space-time is not important when the GW is produced. However, the inflation effect distorts the GW spectrum. As a result, the energy density behaves as

$$\frac{d\rho_{\text{GW}}}{d\log k} \sim k^{-4} \frac{d\rho_{\text{GW}}^{\text{flat}}}{d\log k_p}, \quad (8)$$

where  $k_p = k/a$ , is the physical momentum.  $d\rho_{\text{GW}}^{\text{flat}}/d\log k_p$  is the GW spectrum produced from the same source in the Minkowski space-time. The distortion factor  $k^{-4}$  stems from the  $k^2$  factor in the denominator of Eq. (4).  $d\rho_{\text{GW}}^{\text{flat}}/d\log k_p$  usually decreases as  $k_p^{-r}$ , with  $r = 1$  for bubble collisions [42]. Therefore, for GW produced by approximately instantaneous sources during inflation, the UV part of the spectrum decreases as  $k^{-5}$ . At the same time, due to the uncertainties of both the finite size and the duration, the oscillatory pattern would be smeared out. This finite size effect should also blunt the oscillation pattern in the regime  $|\tau_*|^{-1} < k < \Delta_{\tau,x}^{-1}$ . Detailed simulation is required to determine how the spectrum is smeared. We mimic this effect by replacing the factor  $(\sin k\tau_*/k\tau_* - \cos k\tau_*)^2$  in Eq. (7) with  $(2\Delta)^{-1} \int_{\tau_*-\Delta}^{\tau_*+\Delta} d\tau' (\sin k\tau'_*/k\tau'_* - \cos k\tau'_*)^2$ , where  $\Delta \sim \Delta_{\tau,x}$  embodies the size of the smearing effect.

Combining the above analysis, the general form of the GW spectrum when it is back into the horizon in RD can be written as

$$\frac{d\rho_{\text{GW}}}{d\log k} = \frac{a^4(\tau_{\text{end}})}{a^4(\tau)} \mathcal{S}(k_p) \frac{d\rho_{\text{GW}}^{\text{flat}}}{d\log k_p}, \quad (9)$$

where  $\mathcal{S}(k_p)$  is

$$\mathcal{S}(k_p) = \frac{H_{\text{inf}}^4}{k_p^4} \left\{ \frac{1}{2} + \frac{\cos(2k_p/H_{\text{inf}}) \sin(2k_p\Delta_p)}{4k_p\Delta_p} + \frac{1}{4k_p\Delta_p} \left( \frac{1 - \cos(2k_p/H_{\text{inf}} - 2k_p\Delta_p)}{k_p/H_{\text{inf}} - k_p\Delta_p} - \frac{1 - \cos(2k_p/H_{\text{inf}} + 2k_p\Delta_p)}{k_p/H_{\text{inf}} + k_p\Delta_p} \right) \right\} \quad (10)$$

$\Delta_p = a^{-1}(\tau_*)\Delta$  is the physical size of the source.

**Detectability of the GW signal.** To get the strength and the frequency of the GW today, we need to study a specific model. We assume that the backreaction from the spectator sector that underwent the phase transition to the evolution of the inflaton field is negligible. To have a detectable signal, the latent heat density released during the phase transition should be larger than  $H_{\text{inf}}^4$ . Hence, the plasma, with energy density that can be estimated as  $T_{\text{GH}}^4 \sim H_{\text{inf}}^4/(2\pi)^4$ , is negligible. As a result, the production of the GW is dominated by bubble collisions. A comprehensive description of bubble collision and GW production can be found in Ref. [42]. During bubble collision the parameter  $\beta \equiv -dS_4/dt$  determines the size of the bubble and the wavelength of the GW, where  $S_4$  is the action of the bounce at the end of the phase transition. Here we use  $S_4$  since the phase transition rate is dominated by the quantum tunneling. For the phase transition to complete during inflation, we assume  $\beta \gg H_{\text{inf}}$ . When  $\beta \approx H_{\text{inf}}$ , numerical simulation is needed which is beyond the scope of this work.

In the case of an instantaneous reheating and followed by RD, all the energy of the inflaton field converts into the radiation energy. Hence, today's relative abundance of GW can be written as

$$\Omega_{\text{GW}}(k_{\text{today}}) = \Omega_R \times \mathcal{S}(k) \times \frac{\Delta\rho_{\text{vac}}}{\rho_{\text{inf}}} \frac{d\rho_{\text{GW}}^{\text{flat}}}{\Delta\rho_{\text{vac}} d \log k_p}, \quad (11)$$

where  $\Omega_R$  is today's abundance of radiation,  $\Delta\rho_{\text{vac}}$  is the latent energy density of the phase transition sector. The last factor is the flat space-time spectrum of GW

$$\frac{d\rho_{\text{GW}}^{\text{flat}}}{\Delta\rho_{\text{vac}} d \log k_p} = \kappa^2 \left( \frac{H_{\text{inf}}}{\beta} \right)^2 \Delta(k_p/\beta), \quad (12)$$

where  $\kappa = 1$  if the energy density of the plasma is negligible, and the simulation result shows

$$\Delta(k_p/\beta) = \tilde{\Delta} \times \frac{3.8\tilde{k}_p k_p^{2.8}}{\tilde{k}_p^{3.8} + 2.8k_p^{3.8}}, \quad (13)$$

where  $\tilde{k}_p = 1.44\beta$  and  $\tilde{\Delta} = 0.077$ . In the calculation of the GW spectrum, we use  $\beta^{-1}$  to estimate  $\Delta_p$  in  $\mathcal{S}$ .

Finally, the observed GW frequency is

$$\frac{f_{\text{today}}}{f_*} = \frac{a(\tau_*)}{a_1} \left( \frac{g_{*S}^{(0)}}{g_{*S}^{(R)}} \right)^{1/3} \frac{T_{\text{CMB}}}{\left[ \left( \frac{30}{g_*^{(R)}\pi^2} \right) \left( \frac{3H_{\text{inf}}^2}{8\pi G_N} \right) \right]^{1/4}}, \quad (14)$$

where the superscript  $(R)$  indicates that the values of parameters at reheating temperature. Due to the distortion induced by inflation, the position of the highest peak of the spectrum corresponds to  $k_p \approx H_{\text{inf}}$ . As a result, assuming  $g_{*S}^{(R)} = g_*^{(R)} \approx 100$ , the frequency of highest peak today is

$$\tilde{f}_{\text{today}} = 1.1 \times 10^{11} \text{ Hz} \left( \frac{H_{\text{inf}}}{m_{\text{pl}}} \right)^{1/2} \left( \frac{a_*}{a_1} \right). \quad (15)$$

Take high scale inflation as an instance,  $(H_{\text{inf}}/m_{\text{pl}})^{1/2} \sim 10^{-3} - 10^{-4}$ . Detectors based on the pulsar timing technology, such as EPTA [9], IPTA [10], and SKA [11] are sensitive to GWs with frequencies around  $10^{-8}$  Hz. From Eq. (15), they can probe the GWs produced at the era of about 40 e-folds before the end of inflation as shown by the blue curves in Fig. 3. The space-based detectors, such as LISA [2], eLISA [1], DECIGO [3], BBO [7, 8], ALIA [6], TianQin [4] and Taiji [5], is sensitive to frequencies around  $10^{-2}$  Hz, corresponding to about 20 e-folds before the end of inflation as shown by the magenta and red curves in Fig. 3. The proposed ground-based detectors (e.g. the Einstein Telescope [15] and the Cosmic Explorer [16]) are sensitive to GWs with frequencies around  $10 - 10^4$  Hz, which correspond to about 15 e-folds from the end of inflation. They can detect the signal of the phase transition if  $\beta \approx 2H_{\text{inf}}$ . However, as shown by the purple dotted curve in Fig. 3, the oscillatory feature is expected to be smeared out since  $\Delta_p \sim H_{\text{inf}}^{-1}$ .

**Signals on CMB** If the phase transition happened about 60 e-folds before the end of inflation, it would leave an imprint on the CMB B-mode power spectrum [40]. Since the strength of the GWs depends on  $H_{\text{inf}}$  only through the ratio  $H_{\text{inf}}/\beta$ , as shown in Eqs. (11) and (12), it is possible to see sizable B-mode spectrum from CMB even in low scale inflation models.

We simulate the B-mode power spectra induced by first order phase transitions using the CLASS package [46]. The result is shown in Fig. 4, where  $\beta/H_{\text{inf}}$  and  $\Delta\rho_{\text{vac}}/\rho_{\text{inf}}$  are fixed to be 30 and 0.01. The frequency of GW depends on  $H_{\text{inf}}$ , which we have chosen to be  $H_{\text{inf}} = 10^{12}$  GeV. The solid, dashed and dot-dashed curves are the spectrum for  $N_e = 59, 58$  and  $57$ , respectively. There are small wiggles induced by the oscillatory pattern in the GW power spectrum. Since the spherical harmonics are not orthogonal to the Fourier modes, the oscillatory pattern is smeared. The amplitude of the oscillation is only about 10% of the total. As a comparison, the black dotted curve in Fig. 4 shows the B-mode power spectrum

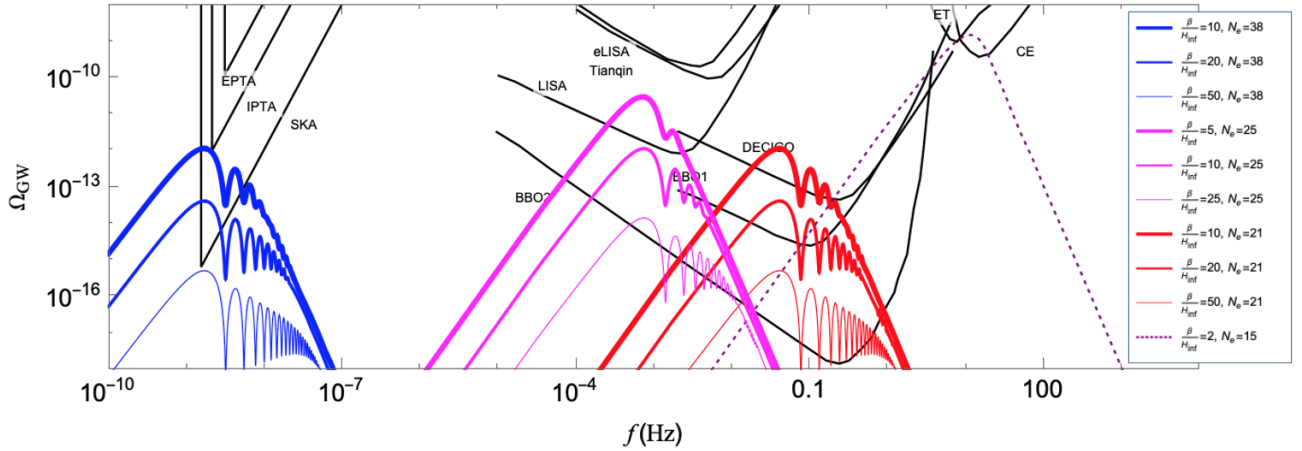


FIG. 3:  $\Omega_{\text{GW}}$  as a function of  $f$ . The blue, magenta, red and purple curves are for  $N_e = 38, 25, 21$  and  $15$ , respectively. The value of  $\beta/H_{\text{inf}}$  for each curve are shown in the legend. For all the curves  $H_{\text{inf}} = 10^{12}$  GeV and  $\Delta\rho_{\text{vac}}/\rho_{\text{inf}} = 0.1$ . The curve for the sensitivity of BBO phase 2 (BBO2) is from [43]. Curves for sensitivities of other detectors are from [44].

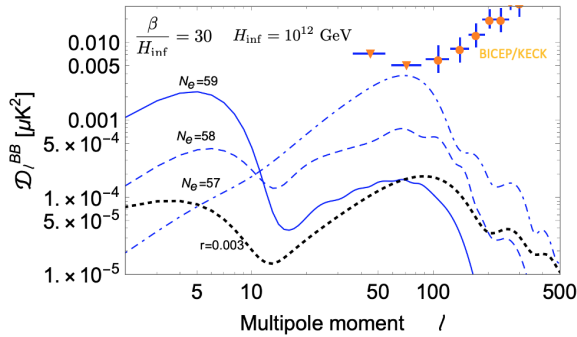


FIG. 4: B-mode power spectra from the bubble collision happened at  $N_e = 59, 58, 57$  during inflation with  $\beta/H_{\text{inf}} = 30$ ,  $H_{\text{inf}} = 10^{12}$  GeV.  $\Delta\rho_{\text{vac}}/\rho_{\text{inf}} = 0.01$ . The spectrum generated from quantum fluctuations for tensor-scalar ratio  $r = 0.003$  is also shown. The orange dots and downward triangles are data from the BICEP/Keck array [45].

produced by quantum fluctuations during inflation with the tensor-scalar ratio  $r = 0.003$ , which can be reached by the CMB-S4 at  $5\sigma$  level [19]. Of course, the inflationary history in this era will also be probed and potentially constrained by other CMB and large scale structure observables. Search for the GW signal discussed here will provide complementary information. We will leave a more detailed discussion to a separate work.

**Summary and outlook** The GW spectrum produced from instantaneous sources during inflation has an oscillatory feature, as shown in Figs. 3 and 4, and can be detected by future GW detectors. This feature allows us to distinguish it from GW generated by sources after the inflation. From the frequency of the oscillation in the spectrum, we can learn the energy scale of the

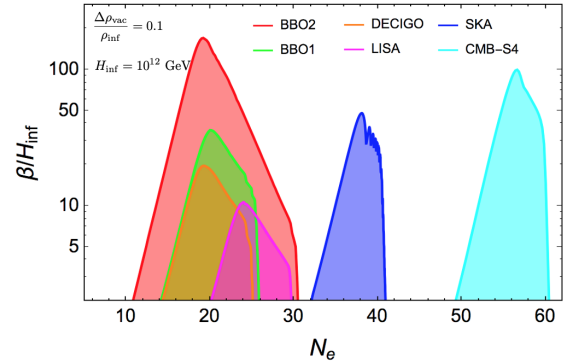


FIG. 5: Reaches of the proposed DECIGO [3], BBO [7], SKA [11] and CMB-S4 [19] projects. For CMB-S4, we require the sum of values of  $D_l^{BB}$  of our spectrum to be smaller than the 0.003 quantum fluctuation spectrum for  $l$  from 50 to 100. For other projects, the reach is set by requiring our signal to be below their sensitivity curves as shown in Fig. 3.

phase transition in the unit of the Hubble expansion rate during inflation. The information of the time the phase transition happened are encoded in the frequency of the GW. Fig. 5 shows the future reaches of LISA, DECIGO, BBO, SKA and CMB-S4 projects for  $\Delta\rho_{\text{vac}}/\rho_{\text{inf}} = 0.1$  and  $H_{\text{inf}} = 10^{12}$  GeV.

For the inflationary history outside the ten e-folds around the CMB era, there is no direct measurement of the power spectrum. Hence, the evolution there could be very different from the simple form assumed in this paper. At the same time, if there is a first order phase transition happened at around  $N_e \geq 10$ , the details of the oscillatory spectrum can help us map out this part of “missing history”. A detailed study of this subject will be presented in a separate work.

If the phase transition happened in the regime that can be detected in CMB, the mass of the fields in the spectator sector must be larger than  $H_{\text{inf}}$  so that their perturbations induced by the phase transition will decay quickly after evolving out of the horizon. On the other hand, if the phase transition happens in the missing history and light degrees of freedom exist in the spectator sector, the perturbations may induce primordial black holes or dark blobs, leading to additional signals in the future.

**Acknowledgement** We thank Yi Wang, Hongliang Jiang, Zhong-Zhi Xianyu and Junwu Huang for useful discussions. HA is supported by NSFC under Grant No. 11975134, the National Key Research and Development Program of China under Grant No.2017YFA0402204 and the Tsinghua University Initiative Scientific Research Program. KFL was supported in part by the National Science Foundation under Grant No. NSF PHY-1748958 and by the Heising-Simons Foundation and acknowledges the hospitality of Kavli Institute for Theoretical Physics while this work was in progress. LTW is supported by the DOE grant DE-SC0013642. The work of SZ was supported in part by the Swedish Research Council under grants number 2015-05333 and 2018-03803.

- 
- [1] P. A. Seoane et al. (eLISA) (2013), 1305.5720.  
 [2] P. Amaro-Seoane et al. (LISA) (2017), 1702.00786.  
 [3] S. Kawamura et al., *Class. Quant. Grav.* **28**, 094011 (2011).  
 [4] J. Luo et al. (TianQin), *Class. Quant. Grav.* **33**, 035010 (2016), 1512.02076.  
 [5] W.-H. Ruan, Z.-K. Guo, R.-G. Cai, and Y.-Z. Zhang, *Int. J. Mod. Phys. A* **35**, 2050075 (2020), 1807.09495.  
 [6] J. Crowder and N. J. Cornish, *Phys. Rev. D* **72**, 083005 (2005), gr-qc/0506015.  
 [7] G. Harry, P. Fritschel, D. Shaddock, W. Folkner, and E. Phinney, *Class. Quant. Grav.* **23**, 4887 (2006), [Erratum: *Class.Quant.Grav.* **23**, 7361 (2006)].  
 [8] V. Corbin and N. J. Cornish, *Class. Quant. Grav.* **23**, 2435 (2006), gr-qc/0512039.  
 [9] M. Kramer and D. J. Champion, *Class. Quant. Grav.* **30**, 224009 (2013).  
 [10] G. Hobbs et al., *Class. Quant. Grav.* **27**, 084013 (2010), 0911.5206.  
 [11] G. Janssen et al., *PoS AASKA14*, 037 (2015), 1501.00127.  
 [12] J. Aasi et al. (LIGO Scientific), *Class. Quant. Grav.* **32**, 074001 (2015), 1411.4547.  
 [13] A. Abramovici et al., *Science* **256**, 325 (1992).  
 [14] F. Acernese et al. (VIRGO), *Class. Quant. Grav.* **32**, 024001 (2015), 1408.3978.  
 [15] M. Punturo et al., *Class. Quant. Grav.* **27**, 194002 (2010).  
 [16] D. Reitze et al., *Bull. Am. Astron. Soc.* **51**, 035 (2019), 1907.04833.  
 [17] H. Hui et al., *Proc. SPIE Int. Soc. Opt. Eng.* **10708**, 1070807 (2018), 1808.00568.  
 [18] H. Li et al., *Natl. Sci. Rev.* **6**, 145 (2019), 1710.03047.  
 [19] K. Abazajian et al. (2019), 1907.04473.  
 [20] L. Grishchuk, *Sov. Phys. JETP* **40**, 409 (1975).  
 [21] A. A. Starobinsky, *JETP Lett.* **30**, 682 (1979).  
 [22] V. Rubakov, M. Sazhin, and A. Veryaskin, *Phys. Lett. B* **115**, 189 (1982).  
 [23] R. Fabbri and M. Pollock, *Phys. Lett. B* **125**, 445 (1983).  
 [24] L. Abbott and M. B. Wise, *Nucl. Phys. B* **244**, 541 (1984).  
 [25] E. Witten, *Phys. Rev. D* **30**, 272 (1984).  
 [26] M. Kamionkowski, A. Kosowsky, and M. S. Turner, *Phys. Rev. D* **49**, 2837 (1994), astro-ph/9310044.  
 [27] T. Vachaspati and A. Vilenkin, *Phys. Rev. D* **31**, 3052 (1985).  
 [28] R. H. Brandenberger, A. Albrecht, and N. Turok, *Nucl. Phys. B* **277**, 605 (1986).  
 [29] M. Hindmarsh, *Phys. Lett. B* **251**, 28 (1990).  
 [30] T. Damour and A. Vilenkin, *Phys. Rev. D* **64**, 064008 (2001), gr-qc/0104026.  
 [31] X. Siemens and K. D. Olum, *Nucl. Phys. B* **611**, 125 (2001), [Erratum: *Nucl.Phys.B* **645**, 367–367 (2002)], gr-qc/0104085.  
 [32] M. Hindmarsh and T. Kibble, *Rept. Prog. Phys.* **58**, 477 (1995), hep-ph/9411342.  
 [33] A. H. Guth, *Adv. Ser. Astrophys. Cosmol.* **3**, 139 (1987).  
 [34] A. D. Linde, *Adv. Ser. Astrophys. Cosmol.* **3**, 149 (1987).  
 [35] A. Albrecht and P. J. Steinhardt, *Adv. Ser. Astrophys. Cosmol.* **3**, 158 (1987).  
 [36] D. Baumann, in *Theoretical Advanced Study Institute in Elementary Particle Physics: Physics of the Large and the Small* (2011), pp. 523–686, 0907.5424.  
 [37] X. Chen and Y. Wang, *JCAP* **04**, 027 (2010), 0911.3380.  
 [38] A. Berera and L.-Z. Fang, *Phys. Rev. Lett.* **74**, 1912 (1995), astro-ph/9501024.  
 [39] A. Berera, *Phys. Rev. Lett.* **75**, 3218 (1995), astro-ph/9509049.  
 [40] H. Jiang, T. Liu, S. Sun, and Y. Wang, *Phys. Lett. B* **765**, 339 (2017), 1512.07538.  
 [41] Y.-T. Wang, Y. Cai, and Y.-S. Piao, *Phys. Lett. B* **789**, 191 (2019), 1801.03639.  
 [42] S. J. Huber and T. Konstandin, *JCAP* **09**, 022 (2008), 0806.1828.  
 [43] G. Harry, <https://dcc.ligo.org/public/0002/G0900426/001/G0900426-v1.pdf> (2009).  
 [44] C. Moore, R. Cole, and C. Berry, *Class. Quant. Grav.* **32**, 015014 (2015), 1408.0740.  
 [45] P. Ade et al. (BICEP2, Keck Array), *Phys. Rev. Lett.* **116**, 031302 (2016), 1510.09217.  
 [46] D. Blas, J. Lesgourgues, and T. Tram, *JCAP* **07**, 034 (2011), 1104.2933.